PROCEEDINGS OF SCIENCE

ATLAS Detector Commissioning with Photons

Thomas Koffas on behalf of the ATLAS Collaboration*
CERN
E-mail: Thomas.Koffas@cern.ch

An intense commissioning activity of the ATLAS detector has preceded the LHC beam start up. The commissioning of the ATLAS detector towards physics with photons has been an integral part of this effort. This paper presents the results of this work, which covers both the photon reconstruction and identification using large-scale simulation samples and smaller-scale samples from specific test-beam data and from in-situ cosmic-ray data.

XXth Hadron Collider Physics Symposium
November 16 – 20, 2009
Evian, France

*Speaker.

PoS(HCP2009)051

1. Photons in the ATLAS Detector

Copious production of photons will be one of the characteristics of the LHC p-p collisions. The main source of isolated high-p_T photons will be QCD processes (direct photon production in association with a jet, or diphotons produced by quark or gluon annihilation). The main background arise from jets misidentified as photons. For physics searches involving photons in the final state therefore, efficient photon reconstruction combined with accurate energy and direction measurement as well as with sufficient jet rejection, will be necessary. Already within the first year of the LHC operation ($\sim 100\,\mathrm{pb}^{-1}$) millions of direct photon and thousands of diphoton events are expected for $E_T > 20$ GeV. Photon statistics will clearly be of no concern in the LHC era, even at the much higher transverse energies of interest for searches for new physics.

1.1 Photon Detection

The two main ATLAS systems used to study photons are the electromagnetic (EM) calorimeter and the tracker. The EM calorimeter is a sampling calorimeter using liquid argon as active material and lead as absorber, covering the pseudorapidity region $|\eta| < 3.2$. The absorber and the electrodes used to collect the ionization charge are longitudinally folded in an accordion shape to obtain a uniform detector in ϕ. In the fiducial region covering $|\eta| < 2.5$, optimized for precision measurements, the calorimeter is longitudinally divided into three layers (called "strips", "middle" and "back"), each highly segmented in $\eta \times \phi$. In front of the first layer and over $|\eta| < 1.8$, a separate layer (presampler) has been installed to correct for dead material energy losses.

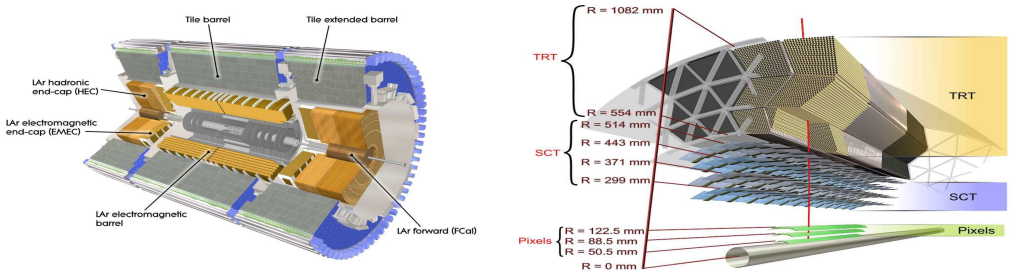

Figure 1: Left:The ATLAS EM and Hadronic Calorimeters. Right: The ATLAS barrel tracker.

The tracker covers $|\eta| < 2.5$ and is operated in a 2 T solenoid field. As shown in Fig. 1, the barrel tracker is composed of three pixel layers, eight strips layers (paired in tilted planes to obtain 4 space points) and a straw tube detector with transition radiation detection capabilities that allows for electron-pion separation. Each of these tracker "barrel" subsystems is complemented by "endcap" (large η) elements, arranged in disks or wheels, to complete the η-coverage (for details see [1]). The total amount of material in the tracker is 0.4 radiation length (X_0) at normal incidence, increasing up to about 2.5 X_0 at $|\eta| = 1.8$.

2. Photon Reconstruction

The ATLAS photon reconstruction algorithm starts by grouping calorimeter cells into clusters. A cluster seed is found when sliding a window of 5×5 cells on the $[\eta \times \phi]$ map of towers with the

collected transverse energy exceeding 3 GeV. The cluster position is then refined around the seed: if there are no prompt tracks pointing to the cluster, the reconstructed object is classified as an unconverted photon and the window is re-sized to 3×5 cells; if there is a conversion (reconstructed by the tracker) pointing to the cluster the window is extended to 3×7 cells to account for the opening of the electron-positron pair in the solenoidal field and for possible energy losses due to bremsstrahlung.

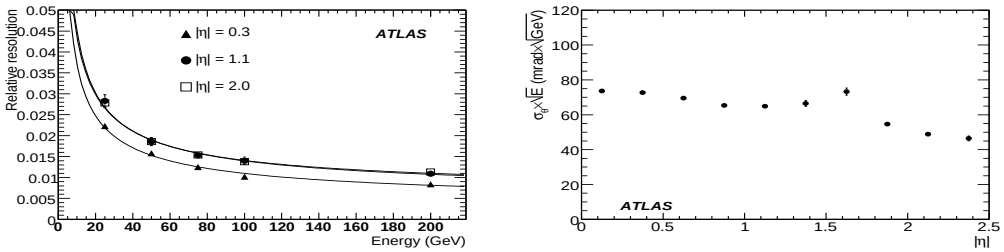

Figure 2: Left: EM calorimeter photon energy resolution for both converted and unconverted photons. Right: Unconverted photon angular resolution as a function of $|\eta|$ (Gaussian fits), multiplied by $\sqrt{E}$.

Efficient conversion vertex reconstruction inside the ATLAS tracker is a fundamental part of the overall photon reconstruction since on average 50% of the photons will convert before reaching the EM calorimeter. First the individual tracks need to be reconstructed. Three tracking algorithms that result in the reconstruction of conversions all the way to the TRT tracker are in place. The vertex reconstruction then follows. The expected radial resolution of the conversion vertices depends strongly on the radial position and is about 3mm for those occurring in the pixel tracker, allowing to resolve most of the tracker structures.

Once the cluster has been classified as electron or photon the cells in the clusters are summed up and energy and position corrections are applied. Converted and unconverted photons receive different energy calibrations (see [2]). These require excellent knowledge of the material in front of the calorimeter. The EM calorimeter linearity $(E_{mean} - E_{true})/E_{true}$ is expected to be within 0.1% for an energy range between 20 and 200 GeV. The relative energy resolution together with the angular resolution of the shower direction for unconverted photons is shown in Fig. 2. The angular resolution for unconverted photons in the energy range of those originating from a H$\rightarrow \gamma\gamma$ decay is accurate enough to contribute only in a small way to the mass resolution, whereas that of converted photons is extracted from the associated tracks and is far superior, namely 0.42 mrad.

3. Photon Identification

The main source of background for high-p_T photons results from QCD jets. The discrimination between photons and jets is based on the observation that photons tend to be narrow isolated objects contained by the EM calorimeter while jets tend to have a broader profile and to deposit a significant amount of energy in the hadronic calorimeter. The corresponding discriminating variables are then the fraction of the shower energy deposited in the hadronic calorimeter and the shower shapes in η and ϕ in the second calorimeter layer. Jets where most of the transverse momentum is taken by a single neutral meson decaying into photons (mainly $\pi^0 \rightarrow \gamma\gamma$) will look like

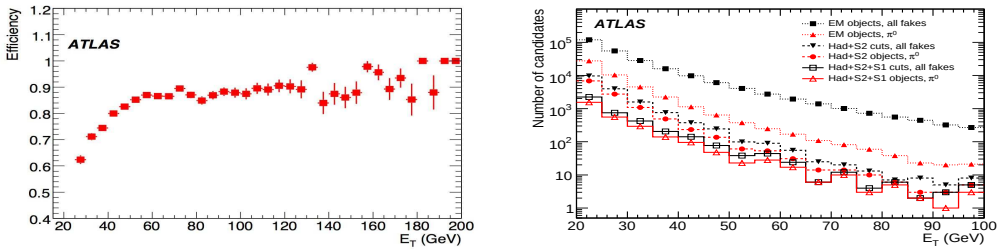

Figure 3: Left:Photon identification efficiency as a function of photon transverse energy. Right:Transverse energy spectrum of fake photon candidates from hadronic jets after varying levels of identification cuts.

isolated photons with respect to these variables. These jets are rejected by using variables built from the finely η-segmented first calorimeter layer ("strips"). Looking at the distribution of the deposited energy in the strips, the photons will appear as a single energy peak confined in a few contiguous strips while the neutral pions will show a characteristic double-peak shape in many cases. Finally the track isolation defined as the sum of the p_T of all tracks (excluding the tracks from the possible photon conversions) with p_T greater than 1 GeV within $\Delta R < 0.3$, where ΔR is the $\eta - \phi$ distance between the track position and the cluster centroid, is also used. A simple cut-based method employing all the cuts above results in a rejection factor of $10^3 - 10^4$ for quark/gluon originating jets, while maintaining a high photon identification efficiency as shown in Fig. 3. The effect of varying identification cuts on the fake photon rejection as a function of E_T is also shown.

4. Photon Identification with Cosmic Rays

During 2008 a considerable amount of cosmic-ray data were collected by the ATLAS collaboration. These data have provided an excellent opportunity in studying the detector response and compare it to the simulation predictions. Of great importance are the shower shape variables that are used for the photon identification. However, there are some limitations. The shower shapes may not correspond to the ones coming from collision-like events. This is particularly true for showers that start at the top of the electromagnetic calorimeter ($\phi > 0$), whereas those starting at the bottom ($\phi < 0$) are more like what one expects during collisions. In addition, cosmic-ray showers are not projective, the energy deposited is rather low in most cases and far fewer candidates are reconstructed in the end-caps.

There are 3.5M events reconstructed in the barrel EM calorimeter. These were compared to 11.5M simulated events. The following cuts were used to select loose or tight projective clusters with energy $E_{cluster}$, well above threshold.

1. $E_{cluster} > 5$ GeV.
2. Loose projectivity: at least one track with impact parameter $|d_0| < 220$ mm and $p_T > 5$ GeV.
3. Tight projectivity for collision-like photon candidates: at least 10% of the total energy deposited in the strips, i.e. $E_{strips} > 0.1 E_{cluster}$

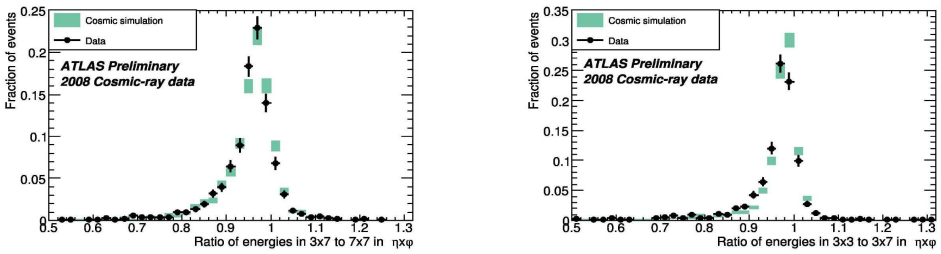

Figure 4: Lateral shower containment along η (left) and ϕ (right), for photon clusters with $E_T > 5$ GeV in the barrel EM calorimeter.

After the above selection 1200 tight projective candidates remain and their shower shape variables were compared to simulation.

The lateral shower containment is at the heart of the photon identification. Along the η-direction this is defined as the ratio of the energy contained in $\Delta\eta \times \Delta\phi = 3 \times 7$ cells over that in 7×7 cells. Along the ϕ-direction it is the ratio of the energy in $\Delta\eta \times \Delta\phi = 3 \times 3$ cells over that in 3×7 cells. These distributions for data and simulation are shown to be in reasonable agreement in Fig. 4.

The fine segmentation of the strip layer is used primarily to reject jets where the majority of the energy is taken by a neutral meson (π^0) decaying into photons. The corresponding lateral shower containment is the discriminating variable in this case. This is defined as $F_{side} = (E_{\pm 3} - E_{\pm 1})/E_{\pm 1}$, i.e. the amount of the cluster energy deposited in the strips, outside the immediate neighbors of the hottest cell, should be small for a prompt photon. This fraction is expected to be different for showers developing from the back of the EM calorimeter ($\phi > 0$) or from the front ($\phi < 0$). This is illustrated in Fig. 5, which displays qualitatively the expected features for this variable with remarkably good agreement between data and simulation.

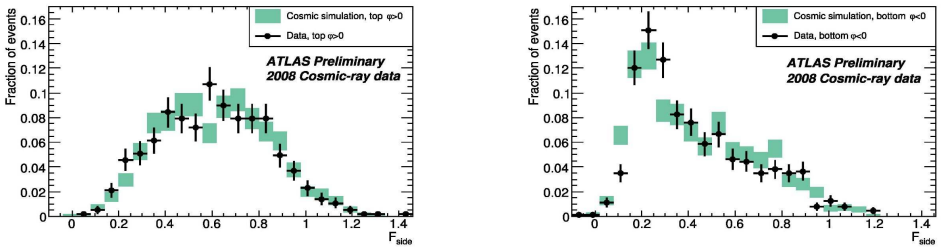

Figure 5: Lateral energy containment for tight projective photon candidates from cosmic-rays (see text). The results are shown separately for $\phi > 0$ (left) and $\phi < 0$ (right).

The above comparisons clearly illustrate the excellent initial understanding of the EM calorimeter response and its description by the simulation. The cosmic-ray results give confidence that the photon identification criteria are adequate in terms of robustness and efficiency.

Table 1: Estimated amount of the material per pixel layer with respect to the Cu foil in front. Statistical and systematic errors are shown for the measurements from data in the first two rows.

	Cu Foil	PixelB	Pixel1	Pixel2
$X/X_0(\%)$	$0.21 \pm 0.02 \pm 0.04$	$1.68 \pm 0.19 \pm 0.35$	$1.95 \pm 0.23 \pm 0.40$	$1.98 \pm 0.24 \pm 0.41$
Ratio	-	$8.16 \pm 1.28 \pm 1.97$	$9.47 \pm 1.51 \pm 2.29$	$9.62 \pm 1.56 \pm 2.26$
$X/X_0(\%)$ in MC	0.25	2.6	2.6	2.6
Ratio in MC	-	10.4	10.4	10.4

5. Material Mapping

One important application of the photon conversions, as was mentioned earlier, is the mapping of the material in the ATLAS tracker. This idea was tested in practice using the Combined Test Beam (CTB) data. Slices of all the ATLAS detectors were placed in a beam line. In particular, tagged photons were then sent through the tracker and the EM calorimeter slices. Due to the lack of adequate statistics only conversions occurring inside the pixel sub-detector have been studied.

A clean set of converted photon candidates was selected by requiring two tracks in the TRT. The number of conversion vertices reconstructed on each pixel layer is then counted. This number is corrected using the reconstruction efficiency estimate versus the conversion position from the simulation. The three pixel layers can clearly be seen as is shown in Fig. 6. The relative amounts of material in each pixel layer with respect to a well known Cu foil placed in front of the pixel tracker, agree well with the expectations from the simulation. A measurement of the absolute amount of the material is more difficult given the large systematic uncertainties on the number of incoming photons. The quantitative results are summarized in Table 1.

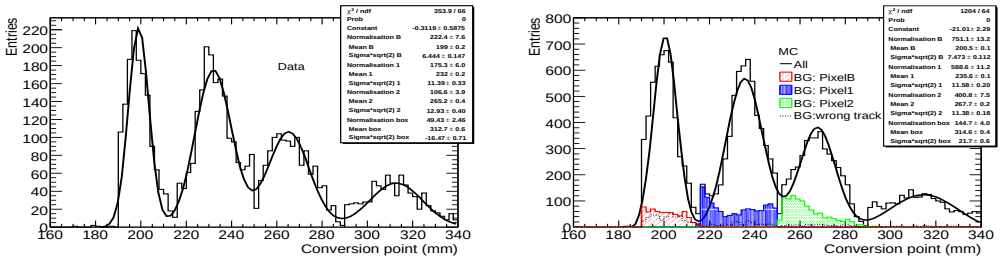

Figure 6: The three pixel tracker layers as seen from the reconstructed photon conversion vertices before any reconstruction efficiency corrections are applied for data (left) and simulation (right).

References

[1] The ATLAS Collaboration, The ATLAS Experiment at the CERN Large Hadron Collider, 2008 JINST 3 S08003.

[2] The ATLAS Collaboration, Expected Performance of the ATLAS Experiment - Detector, Trigger and Physics, arXiv:0901.0512, 2009.